



HAL
open science

Domestic thermoelectric cogeneration drying system: Thermal modeling and case study

Hassan Jaber, Mahmoud Khaled, Thierry Lemenand, Rabih Murr, Jalal Faraj, Mohamad Ramadan

► To cite this version:

Hassan Jaber, Mahmoud Khaled, Thierry Lemenand, Rabih Murr, Jalal Faraj, et al.. Domestic thermoelectric cogeneration drying system: Thermal modeling and case study. *Energy*, 2019, 170, pp.1036-1050. 10.1016/j.energy.2018.12.071 . hal-02171689

HAL Id: hal-02171689

<https://hal.science/hal-02171689>

Submitted on 19 Oct 2021

HAL is a multi-disciplinary open access archive for the deposit and dissemination of scientific research documents, whether they are published or not. The documents may come from teaching and research institutions in France or abroad, or from public or private research centers.

L'archive ouverte pluridisciplinaire **HAL**, est destinée au dépôt et à la diffusion de documents scientifiques de niveau recherche, publiés ou non, émanant des établissements d'enseignement et de recherche français ou étrangers, des laboratoires publics ou privés.



Distributed under a Creative Commons Attribution - NonCommercial 4.0 International License

Domestic Thermoelectric Cogeneration Drying System: Thermal Modeling, and Case Study

Hassan Jaber^{a,c}, Mahmoud Khaled^{a,b}, Thierry Lemenand^c and Mohamad Ramadan^{a,d}

^a *School of Engineering, Lebanese International University LIU, PO Box 146404 Beirut, Lebanon.*

^b *Univ Paris Diderot, Sorbonne Paris Cité, Interdisciplinary Energy Research Institute (PIERI), Paris, France*

^c *LARIS EA 7315, University of Angers – ISTIA, Angers, France*

^d *Associate member at FCLAB, CNRS, Univ. Bourgogne Franche-Comte, Belfort cedex, France.*

Abstract- The demand for enhancing fuel consumption and mitigating exhaust fumes accountable for the greenhouse effect push toward developing efficient energy recovery systems. Optimizing the heat recovery process can be achieved by adding multi-recovery stages. In this frame, the present work suggests a new multi-stage recovery system for heating water and air and generating electricity. The concept of the system is applied to the exhaust gases of a chimney. A complete thermal modeling of the system is drawn. Then a case study is carried out for three different fed fuels (diesel, coal, wood). The results show that when diesel is used water temperature achieved 351 K and 240 W electric power is generated. Moreover, a 0.16 m² heat recovery heat exchanger area is required to heat air to 363 K at an air flow rate of 0.0076 kg/s. Such system can recover up to 84% of the energy lost to the environment when wood is utilized as a fed fuel.

Keywords : Energy, Heat Recovery, Hybrid system, TEG, Cogeneration.

1- Introduction

1.1- Problem background

Nowadays there is an increasing interest in reducing global energy consumption. This interest is caused mainly by high cost of energy sources, high toxic gases emissions, global warming and obligatory governmental laws. The main sources of energy are fossil fuels which are experiencing rapid augmentation in cost, and due to the fact that energy consumption is an effective cost parameter per industrial product, alternative energy has gained significant place in scientist researches shared with effective and efficient benefiting of the available energy [1].

Energy recovery and renewable energy are a suitable solution of such problems [2-7]. The connotation of renewable energy deals with energy captured from a natural renewable source like solar, wind, wave, etc. [8-20], while energy recovery deals with wasted energy from a facility to the environment.

Large number of industrial and residential processes unleashes thermal energy that can be reutilized in order either to increase the efficiency of the system or to become an energy source for different applications [21]. Recovering wasted energy can then increase the efficiency of the system but also reduce pollution and reduce the effective cost of energy. This dissipated energy is mainly released through exhaust gases or cooling water. Many applications have high amount of wasted heat in its exhaust gases that could be recovered such as steam boilers, engines, ovens, chimneys, furnaces, etc. [22-40].

1.2- Heat recovery from exhaust gases

Heat recovery from exhaust gases can be classified according to different taxonomies such as equipment used (heat exchangers), application (source of energy lost), gases temperature or even the suggested purpose of recovery [41]. Figure 1 shows the main recovery goals for heat recovery technology.

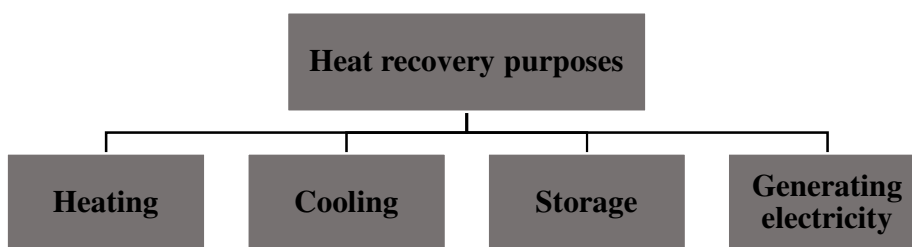


Figure 1. Main aims of heat recovery from exhaust gases.

Khaled et al. [42] did a parametric study on waste heat recovery system from exhaust gases of a 500 kVA generator. They carried out a comparison between having on the one hand, water inside the pipes of a concentric tube heat exchanger and exhaust gases located at the annulus, or on the other hand water inside the annulus and exhaust gases located inside the pipe. For a 0.75 diameter ratio and water flowing inside the tube, 26 kW of thermal energy can be captured by water and this configuration is set as the most efficient one.

Hatami et al. [43] wrote a short review on heat exchangers utilized for heat recovery from diesel engines. This work presented technologies to increase heat transfer on heat exchangers and how can these technologies be applied to transfer heat from exhaust gases of an engine. Also, it presented a complete review about previous heat exchangers used for heat recovery process.

Zhang et al [44] suggested a novel high temperature heat exchanger with hybrid improved technologies to enhance waste heat recovery efficiency. The authors developed algorithm for high temperature heat exchanger structural design and optimization and verified it based on the experimental results. The developed algorithm was used to estimate the heat transfer and pressure drop of the suggested high temperature heat exchanger. It was obtained that the increase in gas temperature and decrease in mass flow rate increase the effectiveness of the proposed high temperature heat exchanger. The average effectiveness of the proposed high temperature heat exchanger and temperature of preheated air are 12.5% and 85.8oC higher than those of the traditional high temperature heat exchanger with additional 70% and 22% pressure drop on air and gas sides respectively.

1.2.1- Water heating

One of the main aims of heat recovery is to benefit from the thermal energy hold by exhaust gases to heat another fluid, solid, or gas. This heating can be performed directly or indirectly. Heating water from exhaust gases thermal energy is exceedingly studied and different systems were suggested and examined.

Khaled et al. [45] developed an experimental analysis on heating water from waste heat of a chimney. A multi-concentric tank is designed in which concentric pipes pass through a water tank. Exhaust gases pass through these pipes allowing heat transfer between exhaust gases and water. The results show 68°C increase in water temperature for only one hour of operation with use of 350°C exhaust gases temperature.

Elgendy and Schmidt [46] studied experimentally the performance of gas engine heat pump integrated with heat recovery subsystem for two modes (At lower air ambient temperature, engine waste heat can be used to evaporate the refrigerant in the refrigerant circuit (mode-I) or to heat the supply water (mode-II)). It was obtained that the influence of condenser water inlet temperature on the system performance is more significant than that of ambient air temperature and engine speed.

Tanha et al [47] studied the performance of drain water heat recovery system and two solar domestic water heaters which are recently installed side-by-side at the Archetype Sustainable Twin Houses at Kortright Center, Vaughan, Ontario. The first solar domestic water heater consists of a flat plate solar thermal collector with a gas boiler and a drain water heat recovery unit, while the second one consists of an evacuated tube solar collector, an electric tank, and a drain water heat recovery unit. It was shown that the drain water heat recovery unit can recover heat of 789 kWh where the effectiveness is about 50%. It was also obtained that the produced annual thermal energy output by the flat plate and evacuated tubes collectors based solar domestic water heater system is respectively 2038 kWh and 1383 kWh.

Ramadan et al. [48] presented a parametric study on heat recovery from the hot air of the condenser to preheat/heat domestic water. The effect of the mass flow rate of air and water was studied. The results show that water temperature can increase to 70°C depending on cooling load and mass flow rate of air. Also, a thermal modeling of the system was performed.

1.2.2- Thermoelectric generators

Thermoelectric generators (TEG) are passive devices used to generate electric power when they are subjected to a temperature gradient at its sides. TEGs are devices that convert thermal energy into electrical energy based on Seebeck effect [49]. Figure 2 shows a schematic for a

thermoelectric module. Such devices are connected thermally in parallel, in which it is sandwiched between a heat source and heat sink, and electrically in series. TEG is a silent, non-vibrating, reliable device with no moving parts. It is a very attractive technology that can be utilized for heat recovery.

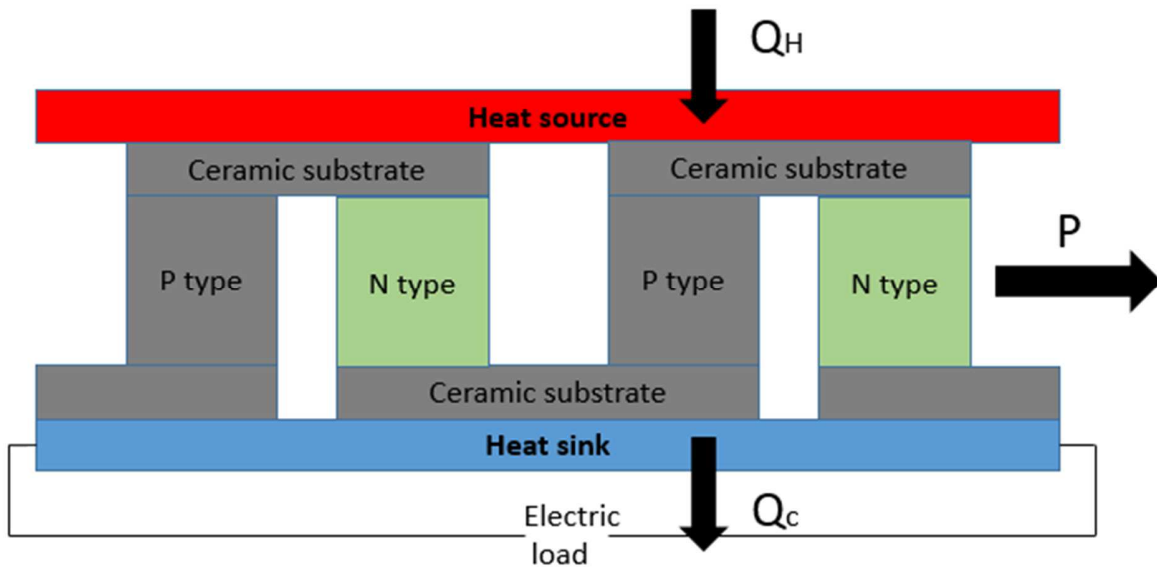


Figure 2. Thermoelectric module.

Huang et al. [50] modeled a three-dimensional thermal resistance analysis to estimate power generated from waste heat recovery system with thermoelectric generators and optimized the suggested system. They obtained that for maximizing the power generation it is required to take into consideration thermoelectric generators position and uniformity of velocity profile. Demira and Dincera [51] conducted new heat recovery system with thermoelectric generators and analyzed numerically the heat transfer of thermoelectric generators. They observed that the inlet temperature and the mass flow rate of exhaust gas entering the system has vital influence on power capacity of the system. Increasing mass flow rate and exhaust gas temperature can

progress power produced by the system by 90%. Besides, rising size of thermoelectric generator by 66.7% lead to increase the overall heat transfer rate of the system by 33.8%. Kim et al. [52] conducted experimental and numerical study of waste heat recovery characteristics of direct contact thermoelectric generator. The output power was estimated and verified using numerical results and empirical correlations. The conversion was between 1-2% and heat recovery efficiencies between 5.7-11.1%. Besides, the efficiency was increased by 0.25% when decreasing coolant temperature by 10°C. Remeli et al. [53] investigated experimentally the combined heat recovery and power generation by using heat pipe assisted with thermoelectric generator system. They obtained that for air velocity equal to 1.1 m/s highest heat exchanger effectiveness of 41% was achieved and the system can recover 1.079 kW of heat and generate about 7 W electric power. Madan et al. [54] designed and fabricated TEGs for low temperature waste heat application utilizing dispenser printing. The produced prototype of the TEG attained output power of 33×10^{-6} W and power density of 2.8 Wm^{-2} with forced convection and pipe surface at 373 K, the output power achieved with natural convection was 8×10^{-6} W.

Shu et al [55] conducted a three-dimensional numerical model of a thermoelectric generator system utilized for engine waste heat recovery. Based on existing model, the study concerned a heat exchanger with thinner wall thickness and moderate inlet dimensions to minimize the negative effects of weight increment and back pressure firstly. The authors then compared the performance of two modes with distinct structures and configurations of thermoelectric modules. It was shown that in single thermoelectric modules, there is a 13.4% increase of maximum power output compared to the original one. While in multi- thermoelectric modules the maximum output power is 78.9 W where there is enhancement of 30.8% compared to the original model. Moreover, it was reported that the fins change the optimal configuration of thermoelectric

modules and increase the maximum output to 89.7 W. Nour Eddine et al [56] investigated the behavior of thermoelectric generator during engine operation and distinguished the impact of the engine flow properties on the performance of thermoelectric generator by designing and constructing three test rigs. The results showed that engine exhaust gas composition and engine exhaust gas pulsation are the two major engine exhaust gas properties that affect the performance of thermoelectric generator. Also, the authors conducted an analytical model to identify and quantify the influence of each parameter on the convective heat transfer coefficient between the exhaust gas and the thermoelectric module, hence on the thermoelectric generator performance. It was obtained that there is difference in the thermoelectric generator output power up to 30% between hot air and real engine test at identical thermoelectric generator inlet temperature and mass flow rate. The model reveals that gas composition is responsible for 5-12% of this difference while another test rig shows that the remaining difference (88-95%) is related to engine exhaust pulsation flow.

1.2.3- Dryers

Dryer are devices used for dehydrating process by applying hot air to remove the moist in food or clothes. In the developed countries, dryers are widely used residentially to dry clothes. Such application is a trend in scientist investments, in which a variety of studies are made on dryers and mainly solar dryers.

Tańczuk et al. [57] developed a research to optimize the size of waste heat recovery heat exchanger which is used for preheating ambient air. Various heat exchanging areas (101–270 m²) were taken under study to simulate their yearly operation concerning several parameters of outlet air and distinct ambient air temperatures. Besides, the authors estimated the energy performance

of the modernization and computed the economic indicators for the analyzed cases. It was concluded that the price of natural gas provided to the system is very effective on the location of optimum of the object in contrast with electricity price which has less influence on it. Han et al. [58] conducted a study to estimate saved energy and water recovery potentials of flue gas pre-dried lignite-fired power system (FPLPS) integrated with low pressure economizer (LPE) for water-cooled units and spray tower (SPT) integrated with heat pump for air-cooled units. The results showed that for optimal LPE scheme, the water recovery ratio was 39.4% and plant efficiency improvement was 0.2%. However, in SPT scheme, the water recovery ratio was 83.3% and heat supply was 110.6 MW. The payback period for both schemes was around 3 years. Walmsley et al. [59] implemented a thermo-economic optimization of industrial milk spray dryer exhaust to inlet air heat recovery. The results of modelling related that spray exhaust heat recovery is very suitable for industrial case study from the economic point of view. Pati et al. [60] analyzed the effect of waste heat recovery on drying characteristics of sliced ginger in a biomass natural convection dryer with sensible heat storage and phase change material. It was found that time needed for phase change material to be melted and the biomass consumed noticeably mitigated when utilizing waste heat. Golman and Julklang [61] developed a simulation code for optimizing the energy usage of spray drying process via exhaust gas heat recovery. It was obtained that when using heat exchanger for exhaust air heat recovery with spray drying system, the energy efficiency increased by 16% and 50% of energy is saved. Jian and Luo [62] proposed a method to reduce energy consumption of domestic venting tumble clothes dryer by using heat recovery. The authors utilized a self-made heat pipe heat exchanger as a recovery unit for domestic venting tumble clothes dryer. The performance of clothes dryer with and without heat recovery was tested and compared under same conditions, including weighing before drying, drying and weighing after drying. It was obtained the exergy and energy efficiencies of the

venting tumble clothes dryer with heat recovery increased respectively from 10.122% to 12.292% and from 47.211% to 57.335% compared to the case of no heat recovery. Also, the electricity consumption reduced 17.606% when heat recovery is used.

1.3- Closure

Jaber et al. [63] did an optimization analysis on a hybrid heat recovery system. This system allows utilizing dissipated exhaust gases to heat water and generate electricity using thermoelectric generators. It is composed of a tank and a tube passes through it, where exhaust gases passes through the tube and water is located in the tank. The study aims to demonstrate the effect of varying the location of TEGs on the performance of the system. Six cases were studied, for which TEGs are located either at the inner or outer surface, of the tank or of the tube, or on all of them. A case study was applied by coupling the recovery system to the exhaust gases of a chimney. It was deduced that water can reach high temperatures (up to 97°C). In addition to that, results show that as the TEGs are located farther from the exhaust gases flow, lower power is generated and higher water temperatures are achieved. When the TEGs are located at all surfaces the total power generated by TEGs is 52 W and hot water attained 81°C. Moreover, an economic and environmental study was performed: it shows that such system hold a 20 months payback period and it is highly affected by the location of TEGs. However, the economic study indicates that changing, the location of TEGs does not affect the amount of CO₂ gas reduced, which is about 6 tons yearly.

Khaled and Ramadan [31] performed a thermal and experimental study on a multi-tube tank heat recovery system (MTTHRS). Exhaust gases generated by a chimney are utilized to heat water using the MTTHRS. The system is composed of a tank and several tubes pass through it, in which exhaust

gases flow through tubes and water is in the annulus. Various experimental tests were done by adjusting the amount of fuel burned. Results showed that in one hour, the temperature of 95 L of water rose by 68°C.

Najjar and Kseibi [64] carry out a theoretical study on a three stages heat recovery system. It utilizes exhaust gases of a stove to generate electricity via TEGs, cook and heat water. A thermal modeling of the system is carried at each stage of the system. Different recovery scenarios were considered by varying the type of fed fuel used (wood, peat and manure). Results show that wood enables the most proper performance of the system, since it produces the highest exhaust gases temperature (920 K) and maximum power generated by 12 TEGs (7.9 W). The overall efficiency of the system was found to be 60% and about 80% of the thermal energy produced from combustion is used by the TEGs and space heating.

Heat recovery has reserved its heavy seat in the research field of scientists. Many studies were done on heat recovery to generate electricity, dry air and heat water but rare they are to combine them in one system. To proceed, the present work suggests a hybrid heat recovery system that recover exhaust gases thermal energy to heat domestic hot water and generate electricity and produces hot air for drying applications. A complete thermal modeling is carried out, starting from the combustion equations till the calculation of gases temperature at each stage. Such system can maximize the energy utilization efficiency, reduce the power consumed residentially and reduce the amount of harmful gases (such as carbon dioxide and carbon monoxide). However, it could increase the pressure drop along the system which will maybe turn off the chimney. Also, such system will suffer from corrosion of the tube, and it requires regular tube cleaning from the flying ashes that could stick on the tube inner surface which reduces the heat transfer rate. This system is coupled with a residential chimney in which exhaust gases produced

from burning fuel for chimney are utilized to enter a domestic thermoelectric cogeneration drying system.

The originality of the work is to suggest new heat recovery system and show using a numerical modelling that it has the potential to be applied in real life. The design of the system is illustrated in section 2. Then a complete thermal modeling for the system is conducted by applying energy balance at each stage of the system (section 3). Section 4 presents a case study in which different fuels are used and studied, the results are compared, analyzed and discussed. And finally a summarizing conclusion of the work is done including future work in section 5.

2- Domestic thermoelectric cogeneration drying system

In this section the suggested thermoelectric cogeneration drying system is illustrated. Figure 3 shows a schematic of the system in which exhaust gases of a chimney pass through a pipe to enter a hybrid heat recovery system, then to a heat recovery heat exchanger and then released to the environment.

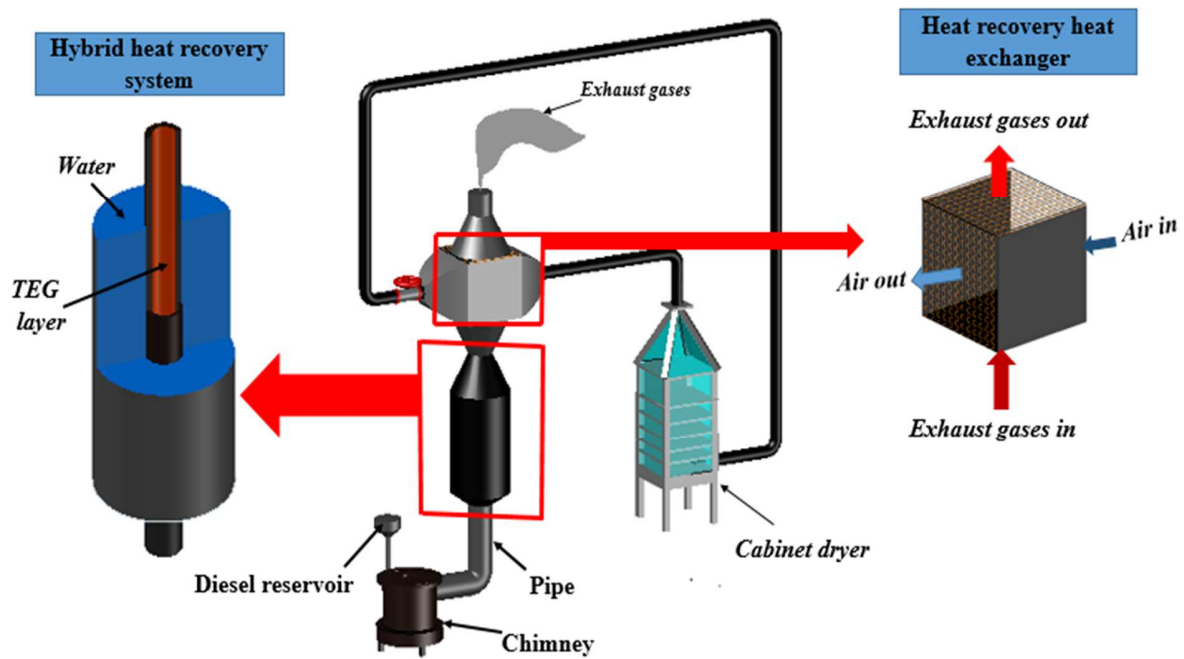


Figure 3. Thermoelectric cogeneration drying system.

This design differs from the conventional system by the two implemented recovery stages: hybrid heat recovery system (HHRS) and heat recovery heat exchanger (HRHE). The main purpose of the hybrid heat recovery system is to absorb part of the thermal energy captured by the exhaust gases to heat domestic hot water and generate electricity. While for the heat recovery heat exchanger, it is utilized to transfer part of the residual thermal energy of the exhaust gases to heat air which is transmitted to a dryer for a drying process (Figure 4).

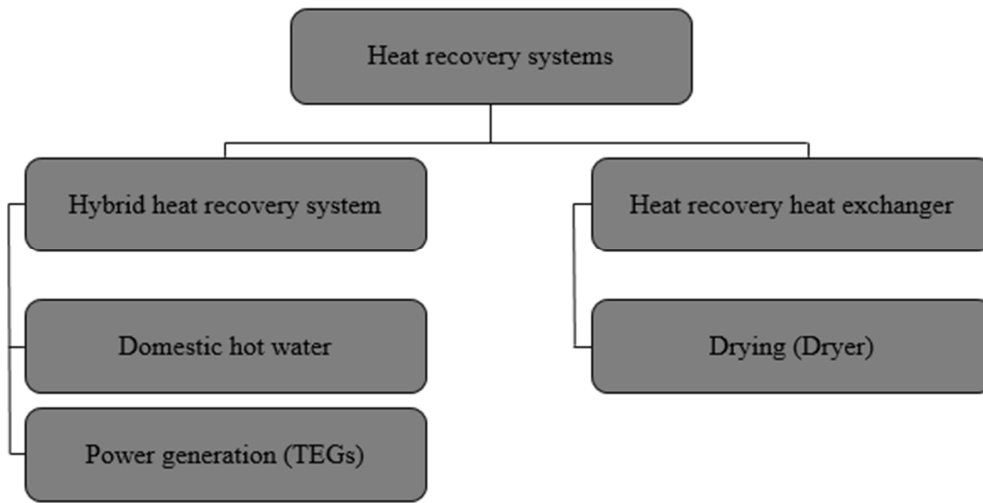


Figure 4. Main purposes of the suggested heat recovery system.

Starting from the combustion of fuel, exhaust gases from combustion process are generated with high thermal energy. Exhaust gases move through a pipe to enter the hybrid heat recovery system through a pipe with TEGs attached to it, in which exhaust gases are in a direct contact with thermoelectric generators. Thermoelectric generators absorb part of the thermal energy captured by exhaust gases where part of it is converted to electric power and the other part transfer to the water surrounding the pipe in a tank heating it. Exhaust gases then enter the heat recovery heat exchanger in which another part of thermal energy is transferred to air heating it. The type of heat exchanger used is an air to air fixed plate heat exchanger. The heated air is then transmitted through pipes by a pump or blower to the dryer where it is used to dry either food or clothes. The remaining thermal energy captured by exhaust gases are released to environment and set as energy losses from the system. It should be noted that the energy lost through the chimney walls, pipes and the hybrid heat recovery system are not set a lost energy since such lost energy is used

to heat the air of the room. The combination of these recovery systems made the overall system named as “domestic thermoelectric cogeneration drying heat recovery system”.

3- System thermal modeling

In order to study the thermal behavior of the system a thermal modeling of the system at each stage is carried. Starting from the combustion of fuel and ending with the released exhaust gases to environment, at each step energy balance is carried out and exhaust gases temperature is studied. Water temperature and power generated by TEG at the hybrid heat recovery system are estimated. Finally, the effect of changing the mass flow rate of air required for drying on the recovery process is studied.

In order to start the thermal modeling, some assumptions should be established:

1. Steady state analysis of the system
2. One dimensional heat transfer.
3. Steady flow of exhaust gases (constant mass flow rate)
4. Constant surface temperature of chimney (between inner and outer)
5. No exhaust gases leakage through all the system.
6. Neglected effect of radiation heat transfer between surfaces and ambient air except at the furnace.
7. No change in the gases convection coefficient through the system
8. Constant ambient air temperature.

In this section, thermal modeling of each part is presented alone [65], showing its energy balance and all related necessary equations in order to obtain the unknowns.

3.1- Furnace

By applying the energy balance at the furnace (Figure 5) the thermal energy released from combustion process through exhaust gases is estimated as follows:

$$\eta_c \cdot Q_f - Q_{L,1} = Q_{gas,1} \quad (1)$$

where Q_f , $Q_{L,1}$ and $Q_{gas,1}$ are respectively, the heat rate generated from burning fuel, heat rate lost from the furnace to the ambient air and heat rate captured by exhaust gases exiting the furnace. η_c is the efficiency of combustion process.

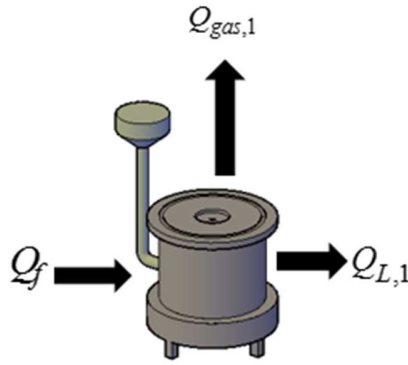


Figure 5. Energy balance at the furnace of the chimney.

The ideal thermal energy produced by burning fuel is function of the lower heat value (*LHV*) of the fuel used:

$$Q_f = \dot{m}_f \cdot LHV \quad (2)$$

where \dot{m}_f is the mass flow rate of fuel (kg/s). This heat rate should be multiplied by the efficiency of combustion to obtain the theoretical heat rate.

Moreover, the exhaust gases heat rate is function of the quantity (\dot{m}_g) and quality ($T_{g,1}$) of exhaust gases:

$$Q_{gas,1} = \dot{m}_g \cdot C_{p_g} \cdot (T_{g,1} - T_a) \quad (3)$$

where \dot{m}_g and C_{p_g} are respectively the mass flow rate and specific heat at constant pressure of exhaust gases. $T_{g,1}$ and T_a are the exhaust gases and ambient air temperatures respectively.

Regarding the lost heat rate ($Q_{L,1}$), the heat rate at the inner ($Q_{L,1,i}$) and outer ($Q_{L,1,o}$) wall of the furnace are equal:

$$Q_{L,1} = Q_{L,1,i} = Q_{L,1,o} \quad (4)$$

The heat transfer at the inner surface of the furnace is composed of convective (Q_{conv}) and radiative (Q_{rad}) parts and expressed as follows:

$$Q_{L,1,i} = Q_{conv} + Q_{rad} \quad (5)$$

$$Q_{L,1,i} = \varepsilon_g \cdot \sigma \cdot A_f (T_{g,1}^4 - T_{s,f}^4) + h_g \cdot A_f \cdot (T_{g,1} - T_{s,f}) \quad (6)$$

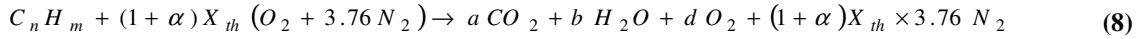
where ε_g and h_g are the emissivity and convection heat transfer coefficient of exhaust gases, A_f is the furnace area, $T_{s,f}$ is the surface temperature of the furnace which is assumed to be constant at the inner and outer sides due to the fact of small thickness of the furnace wall, σ is the Stefan Boltzmann constant.

At the outer side of the furnace the lost heat rate is:

$$Q_{L,1,o} = \varepsilon_f \cdot \sigma \cdot A_f (T_{s,f}^4 - T_a^4) + h_a \cdot A_f \cdot (T_{s,f} - T_a) \quad (7)$$

where ε_f and h_a are the emissivity of the furnace wall and convection heat transfer coefficient of air.

For the combustion process with excess air, the theoretical combustion equation is:



The actual air to fuel ratio $\left(\frac{A}{F}\right)_{act}$ for an excess air fuel combustion process is estimated from

the theoretical air to fuel ratio $\left(\frac{A}{F}\right)_{theor}$, which is the mass of air over the mass of fuel.

$$\left(\frac{A}{F}\right)_{theor} = \left(\frac{m_a}{m_f}\right)_{theor} = \frac{X_{th} \cdot M_{O_2}}{0.23 \times m_f} \left(\frac{kg_{air}}{kg_{fuel}}\right) \quad (9)$$

$$\left(\frac{A}{F}\right)_{act} = (1 + \alpha) \cdot \left(\frac{A}{F}\right)_{theor} \quad (10)$$

$$\left(\frac{m_a}{m_f}\right)_{stoich} = \left(\frac{\dot{m}_a}{\dot{m}_f}\right)_{stoich} \quad (11)$$

where m_a , m_f , \dot{m}_a , \dot{m}_f are the masses and mass flow rate of air and fuel respectively, M_{O_2} is the molar mass of oxygen, α is the percentage of excess of air and X_{th} is the theoretical oxygen to fuel mole fraction which is estimated by stoichiometry. The mass flow rate of air is:

$$\dot{m}_a = \left(\frac{A}{F}\right)_{act} \cdot \dot{m}_f \quad (12)$$

The mass flow rate of exhaust gases released \dot{m}_g is the summation of the mass flow rate of fuel and air:

$$\dot{m}_g = \dot{m}_f + \dot{m}_a \quad (13)$$

3.2 Pipe

By applying energy balance at the pipe shown in Figure 6, we can write:

$$Q_{gas,1} - Q_{L,2} = Q_{gas,2} \quad (14)$$

where $Q_{gas,2}$ and $Q_{L,2}$ are the thermal energy hold by exhaust gases at the outlet of the pipe and the lost thermal energy with air respectively.

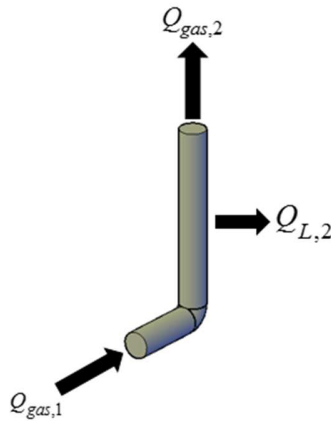


Figure 6. Heat balance at the pipe.

Knowing that the exiting temperature of exhaust gases from pipe is expressed by $T_{g,2}$, the exiting heat rate of exhaust gases is:

$$Q_{gas,2} = \dot{m}_g \cdot Cp_g \cdot (T_{g,2} - T_a) \quad (15)$$

The heat loss rate at the pipe is estimated by the following equation:

$$Q_{L,2} = U_p \cdot A_{p,o} (T_{m,p} - T_a) \quad (16)$$

where U_p is the overall heat transfer coefficient of the pipe, $A_{p,o}$ is the outer area of the pipe and $T_{m,p}$ is the average mean temperature at the pipe, estimated as follows:

$$T_{m,p} = \frac{T_{g,1} + T_{g,2}}{2} \quad (17)$$

The overall heat transfer coefficient is composed of three parts of heat transfer. Starting from the convection heat transfer between gases and internal surface of the pipe ($R_{g,p}$) to the conduction through the pipe (R_p), ending with convection heat transfer between the outer surface of the pipe and air ($R_{p,a}$). It should be noted that the radiative part of heat transfer between pipe surface and ambient air is neglected.

$$U_p \cdot A_{p,o} = \frac{1}{R_{total,p}} = \frac{1}{R_{g,p} + R_p + R_{p,a}} \quad (18)$$

$$U_p \cdot A_{p,o} = \frac{1}{\frac{1}{h_g \cdot A_{p,i}} + \frac{\ln(r_{p,o}/r_{p,i})}{2\pi \cdot K_p \cdot L} + \frac{1}{h_a \cdot A_{p,o}}} \quad (19)$$

where $r_{p,i}$, $r_{p,o}$ and K_p are respectively the inner, outer radii and thermal conductivity of the pipe. The summation of the resistance over the pipe is expressed by $R_{total,p}$. The inner $A_{p,i}$ and outer $A_{p,o}$ areas of the pipe are the lateral areas and calculated as follows:

$$A_{p,i} = 2 \cdot \pi \cdot r_{p,i} \cdot L_p \quad (20)$$

$$A_{p,o} = 2 \cdot \pi \cdot r_{p,o} \cdot L_p \quad (21)$$

By equating the previous equations (3), (14), (15), (16) and (17), $T_{g,2}$ is equal to:

$$T_{g,2} = \frac{T_{g,1} (\beta_p - 0.5) + T_a}{\beta_p + 0.5} \quad (22)$$

where β_p is the multiple of mass flow rate and specific heat of gases at constant pressure and the total resistance over the pipe:

$$\beta_p = \dot{m}_g \cdot C_{p_g} \cdot R_{total,p} \quad (23)$$

3.3- Hybrid heat recovery system – HHRS

When exhaust gases pass out from the pipe, they enter to the first part of the heat recovery process at which domestic hot water is heated and electric energy is generated using TEGs. At the hybrid heat recovery system, the thermal energy that enters the system is splitted: a part of it is transferred to the TEGs then to water and to the ambient air (Q_{sys}) and the other part remains captured by the exiting exhaust gases ($Q_{gas,3}$), Figure 7 illustrates the equation (24).

$$Q_{gas,2} = Q_{sys} + Q_{gas,3} \quad (24)$$

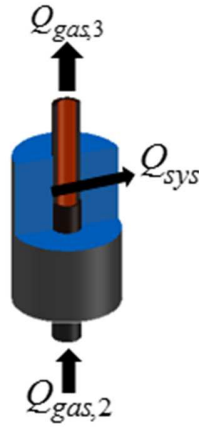


Figure 7. Heat balance for the hybrid heat recovery system

The heat rate at the exit of the system is associated by the following equation:

$$Q_{gas,3} = \dot{m}_g \cdot C_{p_g} \cdot (T_{g,3} - T_a) \quad (25)$$

where $T_{g,3}$ is the exiting temperature of exhaust gases from the system. Due to the presence of the thermoelectric generators, the heat transfer rate through the hybrid heat recovery system is:

$$Q_{sys} = Q_{L,3} + P \quad (26)$$

where $Q_{L,3}$ and P are the heat loss rate with ambient air and the power generated by TEGs. At the TEG, the power produced is the difference of the thermal energies at the heat source and sink sides.

$$P = Q_H - Q_C \quad (27)$$

It should be noted that Q_H is equal to Q_{sys} and Q_C is equal to Q_{L3} . From the electrical modeling part of thermoelectric generators, the following equations are raised showing a direct relationship between the power and the temperature difference at the TEG sides.

$$Q_H = N \left\{ U_{PN}(T_H - T_C) + \alpha \cdot I \cdot T_H - \frac{I \cdot R_i^2}{2} \right\} \quad (28)$$

$$Q_C = N \left\{ U_{PN}(T_H - T_C) + \alpha \cdot I \cdot T_C - \frac{I \cdot R_i^2}{2} \right\} \quad (29)$$

$$P = \alpha \cdot I (T_H - T_C) - I \cdot R_i^2 \quad (30)$$

$$I = \frac{\alpha(T_H - T_C)}{2R_i} \quad (31)$$

In order to simplify the calculation, and since the maximum energy conversion efficiency of TEG is about 5%, the TEG layer is represented as a layer having its own thermal resistance with a constant heat flow rate across the system. In other words, since the power generated P is very small compared to the heat transfer rate across the system (Q_{sys}), then the heat transfer rate is assumed to be constant over the system allowing to initialize the following equations.

$$Q_{sys} = U_{sys} \cdot A_{t,o} \cdot (T_{m,sys} - T_a) \quad (32)$$

where U_{sys} and $T_{m,sys}$ are respectively the overall heat transfer coefficient of the HHRS and the average mean temperature at the HHRS, and $A_{t,o}$ is the outer area of the tank. The average mean temperature is function of the entering and exiting exhaust gases temperature from the system:

$$T_{m,sys} = \frac{T_{g,2} + T_{g,3}}{2} \quad (33)$$

The overall heat transfer coefficient is estimated by the type of heat transfer and its relative area.

$$U_{sys} \cdot A_{sys,o} = \frac{1}{R_{total,sys}} = \frac{1}{R_{g,sys} + R_{TEG} + R_{tube} + R_{tu-w} + R_{w-t} + R_t + R_{a,sys}} \quad (34)$$

$$U_{sys} \cdot A_{sys,o} = \frac{1}{\frac{1}{h_g \cdot A_{TEG,i}} + \frac{\ln(r_{TEG,o}/r_{TEG,i})}{2\pi \cdot K_{TEG} \cdot L} + \frac{\ln(r_{tu,o}/r_{tu,i})}{2\pi \cdot K_{tu} \cdot L} + \frac{1}{h_w \cdot A_{tu,o}} + \frac{1}{h_w \cdot A_{t,i}} + \frac{\ln(r_{t,o}/r_{t,i})}{2\pi \cdot K_t \cdot L} + \frac{1}{h_a \cdot A_{t,o}}} \quad (35)$$

where the total resistance over the HHRS ($R_{total,sys}$) is composed of convection resistance between gases and TEG surface ($R_{g,sys}$), conduction through the TEG (R_{TEG}) and tube (R_{tube}), convection between outer tube surface and water (R_{tu-w}) and convection between water and inner tank's wall (R_{w-t}), conduction over the tank wall (R_t) and finally convection between outer tank surface and ambient air ($R_{a,sys}$). K_{TEG} , K_{tu} and K_t are the conduction coefficients of the TEG layer, tube and tank respectively. Due to the small size of TEG it is assumed as tubular shape then the inner and outer areas are:

$$A_{TEG,i} = 2 \cdot \pi \cdot r_{TEG,i} \cdot L_s \quad (36)$$

$$A_{TEG,o} = 2 \cdot \pi \cdot r_{TEG,o} \cdot L_s \quad (37)$$

where $r_{TEG,i}$ and $r_{TEG,o}$ are the inner and outer radii of the TEG, and L_s is the longitudinal length of the HHRS. The inner and outer area of the tube and tank are calculated as follow:

$$A_{tu,i} = 2 \cdot \pi \cdot r_{tu,i} \cdot L_s \quad (38)$$

$$A_{tu,o} = 2 \cdot \pi \cdot r_{tu,o} \cdot L_s \quad (39)$$

$$A_{t,i} = 2 \cdot \pi \cdot r_{t,i} \cdot L_s \quad (40)$$

$$A_{t,o} = 2 \cdot \pi \cdot r_{t,o} \cdot L_s \quad (41)$$

where $r_{tu,i}$, $r_{tu,o}$, $r_{t,i}$ and $r_{t,o}$ are the inner and outer radii of the tube and tank respectively. Then the exiting exhaust gases temperature $T_{g,3}$ is:

$$T_{g,3} = \frac{T_{g,2} (\beta_{sys} - 0.5) + T_a}{\beta_{sys} + 0.5} \quad (42)$$

where β_{sys} is a constant equated to:

$$\beta_{sys} = \dot{m}_g \cdot C_{p_g} \cdot R_{total,sys} \quad (43)$$

The average water temperature is measured at the average position (mid position) and estimated by the following equation:

$$T_{w,avg} = T_{tu,o} - Q_{sys} \cdot R_{tu-w} \quad (44)$$

where $T_{tu,o}$ is the temperature of the outer surface of the tube.

The power produced per one TEG (P_{1TEG}) is directly proportional to the square of the temperature difference at the TEG (ΔT^2):

$$P_{1TEG} = \left(\frac{P}{\Delta T^2} \right)_{ref} \cdot \Delta T^2 \quad (45)$$

where $\left(\frac{P}{\Delta T^2}\right)_{ref}$ is the reference ratio of power generated for a specific square of temperature difference provided by the manufacturer. The total power produced by TEGs (P_{total}) is estimated by multiplying the power produced by one TEG with N_{TEG} the number of TEGs available at the pipe.

$$P_{total} = N_{TEG} \cdot P_{1TEG} \quad (46)$$

3.4- Dryer

After the first part of the energy lost is recovered at the HHRS, exhaust gases enter to the second part of heat recovery process in which air is heated to be used in drying process. A counter flow fixed plate air to air heat recovery heat exchanger is utilized (Figure 8). Such heat exchanger is characterized by large heat exchange area which is a crucial parameter in air to air heat recovery process. The outlet air temperature and the mass flow rate of air are suggested in order to calculate the required heat exchange area.

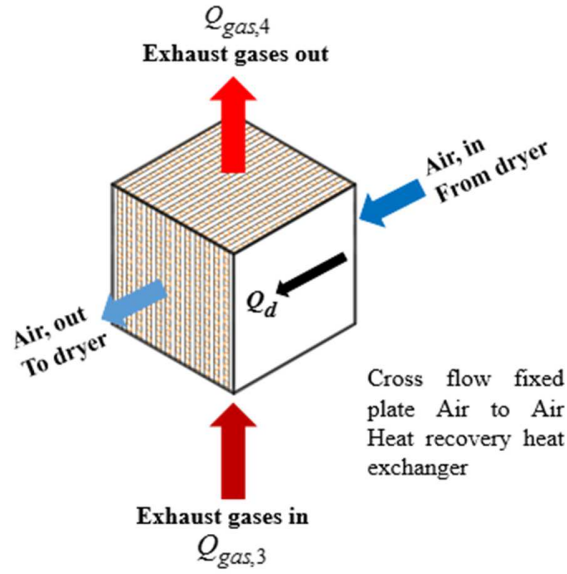


Figure 8. Fixed plate air to air heat exchanger.

By applying the thermal energy balance at the heat recovery heat exchanger (HRHE) shown in Figure 8, the following equations are raised:

$$Q_{gas,3} = Q_{HRHE} + Q_{gas,4} \quad (47)$$

$$Q_{gas,4} = Q_{H,HE} = \dot{m}_g \cdot Cp_g \cdot (T_{g,4} - T_a) \quad (48)$$

$$Q_{C,HE} = \dot{m}_a \cdot Cp_a \cdot (T_{a,o} - T_a) \quad (49)$$

$$Q_{H,HE} = Q_{C,HE} = U_{HE} \cdot A_{HE} \cdot \Delta T_{lm} \quad (50)$$

where Q_{HRHE} is the heat transfer rate to heat exchanger, $Q_{gas,4}$, $Q_{H,HE}$ and $Q_{C,HE}$ are the sensible heat rate exiting the heat exchanger, hot and cold stream heat transfer rate at the heat exchanger respectively, \dot{m}_a , $T_{g,4}$ and $T_{a,o}$ are the mass flow rate of air, exiting exhaust gases and air

temperature from the heat exchanger, and ΔT_{lm} is the logarithmic mean temperature difference, calculated as follows:

$$\Delta T_{lm} = \frac{\Delta T_{out} - \Delta T_{in}}{\ln(\Delta T_{out} / \Delta T_{in})} = \frac{(T_{g,4} - T_{a,o}) - (T_{g,3} - T_a)}{\ln\left(\frac{T_{g,4} - T_{a,o}}{T_{g,3} - T_a}\right)} \quad (51)$$

where U_{HE} and A_{HE} are the overall heat transfer coefficient and the heat exchange area of the heat exchanger. The overall heat transfer coefficient is composed of convection heat transfer of the hot stream and plate's surface and conduction heat transfer through the heat exchanger plate and convection heat transfer between the plate and cold stream.

$$\frac{1}{U_{HE}} = \frac{1}{h_h} + \frac{t_{plate}}{K_{plate}} + \frac{1}{h_c} \quad (52)$$

where h_h and h_c are the convection coefficients of the hot and cold stream, t_{plate} and K_{plate} are the thickness and conduction coefficient of the plates. The area of a fixed plate heat exchanger is defined by the number of plates N_{plates} , multiplied by the height H_{plate} and width W_{plate} of the plate:

$$A_{HE} = N_{plates} H_{plate} \cdot W_{plate} \quad (53)$$

4- Case study and results

Diesel, coal and wood chimney are the main types of chimneys utilized residentially. They are different in the shape of the furnace (coal and wood include ash drawer) and residues coming out of burning. The gases flow rate of diesel chimney is steadier than coal and wood chimneys, due

to the simplicity in controlling the amount of fuel added in diesel and hardness of maintaining constant rate of adding wood for wood chimneys. As presented above, the flow rate of fuel is assumed constant in this study.

4.1- Furnace

The three types of fuel are considered in this study in order to check the effect of changing the fuel used in burning on the behavior of the double stage hybrid heat recovery system. Specific types of diesel, coal, and wood are selected with its corresponding molecular formula. The theoretical chemical combustion equations are shown in the Table 1.

Table 1. Theoretical chemical combustion equation for the different types of fuel.

Type of fuel	Theoretical chemical combustion equation
Diesel	$C_{12}H_{23} + X_{th}(O_2 + 3.76N_2) \rightarrow aCO_2 + bH_2O + X_{th} \times 3.76N_2$
Coal	$\frac{84.7}{12}C + \frac{2.9}{2}H_2 + \frac{1.5}{28}N_2 + \frac{1.6}{32}O_2 + \frac{0.8}{32}S + X_{th}(O_2 + 3.76N_2) \rightarrow aCO_2 + bH_2O + dSO_2 + kN_2$
Wood	$\frac{50}{12}C + \frac{6}{2}H_2 + \frac{42}{32}O_2 + \frac{1}{28}N_2 + others + X_{th}(O_2 + 3.76N_2) \rightarrow aCO_2 + bH_2O + kN_2 + others$

In the equations of Table 1, the constants a, b, d, k are evaluated from stoichiometry by applying mole balance for carbon, hydrogen, oxygen and others. Table 2 recapitulates the values of these constants and the corresponding theoretical air to fuel ratio calculated using equation (9) and the

actual air to fuel ratio with a 30% excess air combustion process (equation 10). Diesel fuel has the highest air to fuel ratio which is due to the molecular formula of diesel.

Table 2. Stoichiometric constants, theoretical and actual air to fuel ratio.

Type of fuel	a	b	d	k	X_{th}	$\left(\frac{A}{F}\right)_{theor}$ (kg _{air} /kg _{fuel})	$\left(\frac{A}{F}\right)_{act}$ (kg _{air} /kg _{fuel})
Diesel	12	11.5	-	-	17.75	24.69	32.1
Coal (Anthracite)	7.058	1.45	0.025	29.22	7.758	10.8	14.04
Wood	4.16	3	-	16.39	4.35	6.05	7.86

Table 3 recapitulates for each type of fuel its corresponding lower heat value with a constant mass flow rate of fuel for all types (1.1 kg/hr). For a 60% combustion efficiency the thermal energy generated by burning fuel is also shown in the Table 3. Diesel exhibits the highest lower heating value which implies higher thermal energy generated and higher thermal energy carried by exhaust gases.

Table 3. Lower heat value, mass flow rate and thermal energy of fuel.

Type of fuel	LHV (MJ/kg)	\dot{m}_f (kg/hr)	η_c	$\eta_c \cdot Q_f$ (W)
Diesel	43.41	1.1	0.6	7958
Coal (Anthracite)	28.74	1.1	0.6	5269
Wood	14.52	1.1	0.6	2662

The main parameters utilized in the thermal modeling of the furnace are given in the following Table 4.

Table 4. Main parameters for furnace modeling.

Parameter	Value		Unit
	Diesel	Coal – Wood	
Furnace surface area (A_f)	0.13	0.18	m ²
Convection coefficient of gases (h_g) [64]	10		W/m ² .K
Specific heat of gases at constant pressure (Cp_g)	1140		kJ/kg.K
Convection coefficient of air (h_a) [64]	20		W/m ² .K
Ambient air temperature (T_a)	298		K
Exhaust gases emissivity (ϵ_g)	0.067		-
Furnace outer surface emissivity (ϵ_f)	0.46		-

Using those parameters and the equations of the furnace the thermal energy lost with ambient air and thermal energy captured by exhaust gases are estimated, knowing that the mass flow rate of

exhaust gases is estimated using equation (13). The main results for the furnace part are summarized in the Table 5.

Table 5. Main results for furnace part.

Type of fuel	$\eta_c \cdot Q_f$ (W)	\dot{m}_g (kg/hr)	$T_{g,1}$ (K)	$Q_{gas,1}$ (W)	$T_{s,f}$ (K)	$Q_{L,1}$ (W)
Diesel	7958	35.31	930	7066	531	886
Coal	5269	15.44	1041	3632	584	1622
Wood	2662	8.64	879	1603	507	1071

Diesel produces the highest quantity of exhaust gases (about three times what wood produce) but not the highest temperature: even though coal has the highest exhaust gases temperature but diesel exhaust gases has the highest thermal energy because it is dependent on mass flow rate and temperature of exhaust gases. Since coal and wood chimneys are larger in area then the heat lost with ambient air is higher than for diesel chimney. Also since coal chimney produces highest exhaust gases temperature then the furnace outer temperature is highest, leading to high energy loss with ambient air. Table 5 shows that for diesel chimney about 11% of the generated thermal energy is dissipated to the surrounding, however for coal and wood chimney the thermal energy lost are 30% and 40% respectively. This is mainly caused by a lower quantity of exhaust gases (mass flow rate) and larger furnace area. It is obvious from the mass flow rate of exhaust gases and for the same size of the pipe, Diesel exhaust gases will flow faster than coal and wood which means that less energy can be recovered in diesel. While for wood case, exhaust gases flow in a lower speed allowing more heat transfer and more percentage of energy recovered compared to

diesel system. Whereas, since exhaust gases flow with low speed it is expected that flying ashes will stick more in wood and coal cases compared to diesel system. The temperature of exhaust gases generated from wood is 96% compatible with the results conducted by Najjar and Kseibi [64].

4.2- Pipe

Exhaust gases flow out from the chimney furnace to the HHRS through a pipe. At the pipe, exhaust gases lose part of their thermal energy to ambient air. The pipe equivalent length is 350 mm including the elbow. The inner and outer radii of the pipe are 50 mm and 51 mm respectively. The conductivity heat transfer of the pipe which is made of iron is 50 W/m.K. By applying the energy balance and the equations related to pipe part, the following results are obtained and recapitulated in Table 6.

Table 6. Main results from pipe part.

Type of fuel	$R_{total,p}$ (K/W)	$T_{g,2}$ (K)	$Q_{gas,2}$ (W)	$Q_{L,2}$ (W)
Diesel	1.355	899	6609	451
Coal	1.355	937	3132	509
Wood	1.355	740	1211	378

As in the furnace, coal chimney loses more thermal energy than diesel and wood ones due to the highest exhaust gases temperature. The total resistance is constant for the three types of fuel

because the dimensions of the pipe are constant for the three cases. From Tables 5 and 6, exhaust gases lose about 3% of its temperature when diesel is used, they decrease 9% when coal is utilized and reduce maximum when wood is utilized (15%). This decrease is mainly caused by low amount of exhaust gases when wood is utilized as a fuel of the chimney. 31% of the energy entering the pipe is lost when wood is utilized, only 16% is lost when coal is used and minimum losses are checked when diesel is used (7%). The main role of a chimney is to heat ambient air in cold weather. The heat is transferred from the combustion chamber to the air through the walls of the chimney. Also, the pipe can transfer heat to the air, then the thermal energy transferred to the air from the pipe wall is not considered as dissipated energy. Since coal has the highest $Q_{L,2}$ then, it heats the ambient air more than the wood and diesel at the pipe stage.

4.3- Hybrid heat recovery system – HHRS

At the HHRS exhaust gases release part of its thermal energy to the recovery system, producing domestic hot water and generating electricity by a thermoelectric cogeneration system. As shown in the design of the HHRS the exhaust gases are in a direct contact with TEG surface. The main parameters of the designed hybrid heat recovery system are summarized in the Table 7.

Table 7. Main parameters for HHRS thermal modeling.

Parameter	Value	Unit
Length of the system	1	m
Inner radius of the tube	0.050	m
Outer radius of the tube	0.051	m
Inner radius of the tank	0.249	m
Outer radius of the tank	0.25	m
Area of TEG	0.003136	m ²
Thickness of TEG	5	mm
Number of TEG available	100	–
K_{TEG}	0.18	W/m.K
K_{tu} (Copper)	401	W/m.K
K_t (Iron)	50	W/m.K
h_w	20	W/m ² .K

Using the thermal modeling equation of the HHRS aforementioned, the main results of the thermal behavior of the system are recapitulated in Table 8.

Table 8. Main results obtained for the HHRS.

Type of fuel	$R_{total,sys}$ (K/W)	$T_{g,3}$ (K)	$Q_{gas,3}$ (W)	Q_{sys} (W)	P_{total} (W)	$T_{w,avg}$ (K)	$Q_{L,3}$ (W)
Diesel	0.667	815	5777	832	240	351	832
Coal	0.667	767	2301	831	240	351	831
Wood	0.667	550	690	521	94	331	521

The hybrid heat recovery system utilized 12.5% of the energy entering the system when diesel is used to produce hot water and generate electricity. This used energy produced 78°C hot water and generated 240 W from 100 TEGs. When coal is used 26.5% of the entering energy is utilized producing the same water temperature and power as when diesel is used. However, when using wood as a fed fuel of the chimney 43% of the entering energy is transfer to the hybrid heat recovery system producing about 58°C hot water and generated 94 W electric power from TEG layer. The main reason of having the same water temperature and power produced for the diesel and coal cases is that the mean temperatures are the same as shown in the Table 9. Since electric water heater is the highest consumer of electric power residentially which increases the electric bill, this stage saves money and reduce the amount of CO₂ gas released to generate the required electricity. Diesel and coal will save money more than wood system does. However, coal system could experience more corrosion phenomenon compared to diesel case since it has lower gases temperature. One hundred TEGs are attached to the tube on the system. The power generated by one TEG for the wood system is around 0.94 W. Najjar and Kseibi [64] estimated that the power generated by one TEG is about 0.7 W.

Table 9. Temperature distribution over the HRS.

Type of fuel	$T_{m,sys}$ (K)	T_H (K)	T_C (K)	$T_{tu,o}$ (K)	$T_{w,avg}$ (K)	$T_{t,i}$ (K)	$T_{t,o}$ (K)	T_a (K)
Diesel	852	558	480	480	351	324	324	298
Coal	852	558	480	480	351	324	324	298
Wood	645	461	412	412	331	31	314	298

In the Table 9, the temperatures $T_H, T_C, T_{t,i}, T_{t,o}$ are respectively the hot and cold temperatures at the TEG and the inner and outer temperatures of the tank wall. It should be noted that T_C is equal to the inner surface temperature of the pipe and due to small thickness of the pipe the temperatures before and after pipe wall or before and after tank wall are the same.

4.4- Dryer

In this part of the system, air to air heat recovery heat exchanger is utilized. There are many types of air to air heat exchanger that can be utilized. Heat pipe, run around coil, rotatory wheel and fixed plate heat exchanger are the main types used. In the present work, fixed plate heat exchanger is used, it has no moving parts and consists of alternated plates, separated and sealed which form the exhaust and supply airstream passages. Fixed plate heat exchanger transfer only sensible heat but they are easy to be cleaned from ashes residues.

The effect of changing the mass flow rate on the required heat exchanger area is studied. In order to estimate the required heat transfer area of the heat exchanger the outlet air temperature is selected to be equal to 363 K. A range of the mass flow rate of air between 0.0001 kg/s to 0.0076

kg/s has been considered with an increment of 0.0003. The heat exchanger plate is made up of copper of cross sectional area of 20×5 cm. The effect of changing the air flow rate on the exhaust gases temperature, area and number of plates required is showed on Figure 9.

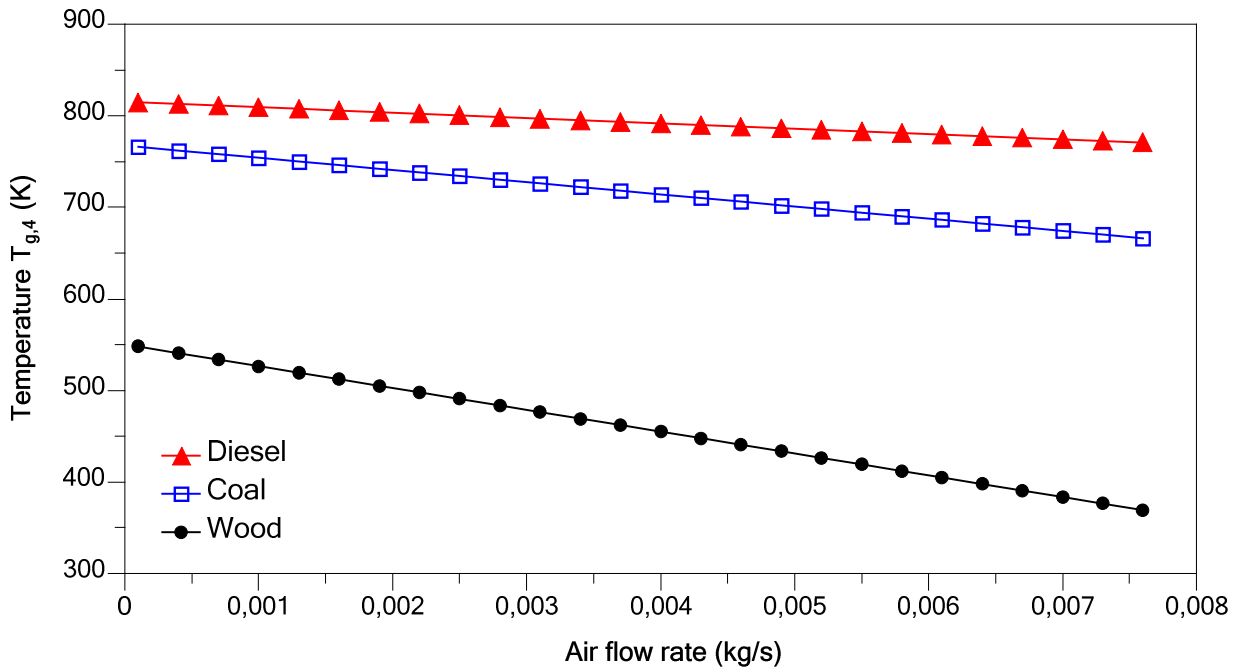


Figure 9. Exiting gases temperature ($T_{g,4}$).

From the Figure 9, as the mass flow rate of air is increased, the outlet exhaust gases temperature is decreased. The Diesel exhaust gases temperature is not highly affected by the change of the air mass flow rate, it is 814 K at 0.0001 kg/s and decreased to 770 K at 0.0076 kg/s (decrease of 44°C), this results from the high thermal energy captured by the entering gases. While for the coal exhaust gases, it experienced a 100°C decrease in temperature with the same increase of air flow rate. At least, exhaust gases of the wood case are the most affected by increasing the air flow rate: the exhaust gases temperature is 547 K at 0.0001 kg/s and decreased at 369 K at 0.0076 kg/s (decrease of 178°C).

The heat exchanger area required is shown in Figure 10 and is directly affected by changing the mass flow rate. Diesel and coal cases are slightly affected compared to the wood case. This is because of the relatively close value of the entering thermal energy of exhaust gases and the required thermal energy transferred to air. At a 0.0076 kg/s flow rate, the area required is 0.16, 0.19 and 1.11 m² for diesel, coal and wood respectively.

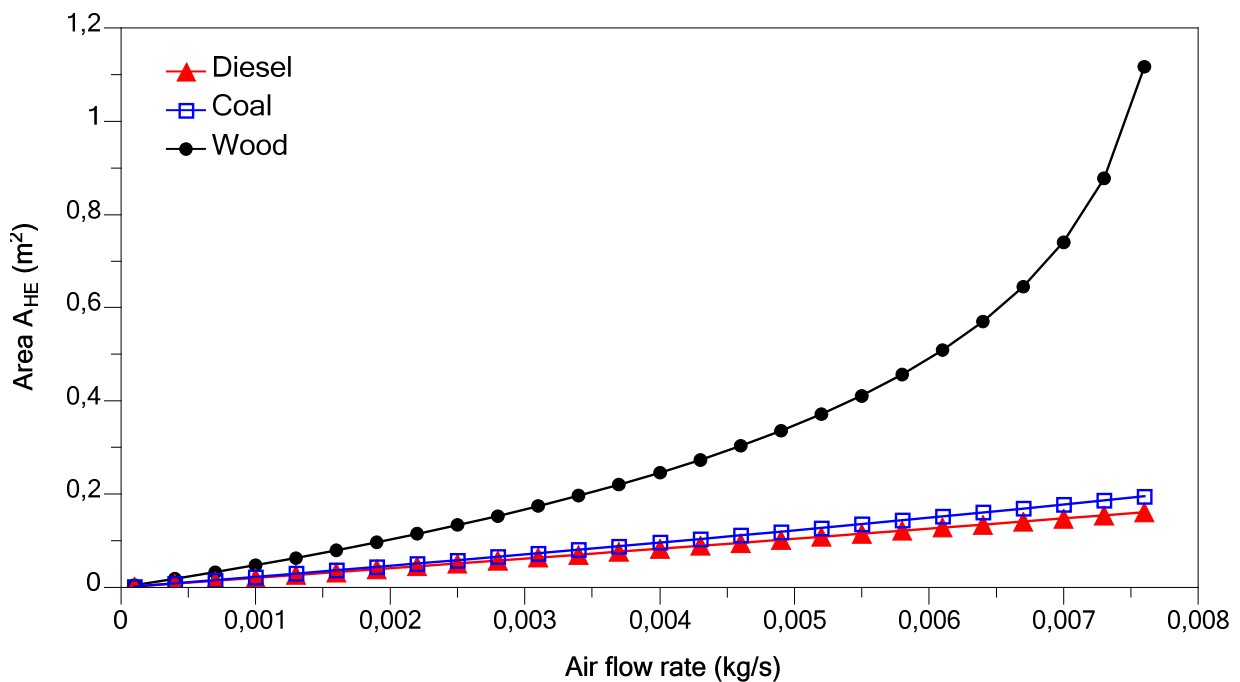


Figure 10. Heat exchanger required area (A_{HE}).

The number of plates is proportional to the area, and with constant width and height (20×5 cm) the change in the number of plates, plots in Figure 11, evolves as the change in the area. At 0.0076 kg/s about 17 plates are required when diesel is used, 20 plates for coal case and 112 plates when wood is used as the fed fuel of the chimney. This implies that as the flow rate of air increases, more plates are required which increases the cost of the heat exchanger especially for

wood system. Increasing the number of plates will also increase the pressure drop which will increase the probability of overstock of ashes on heat exchanger.

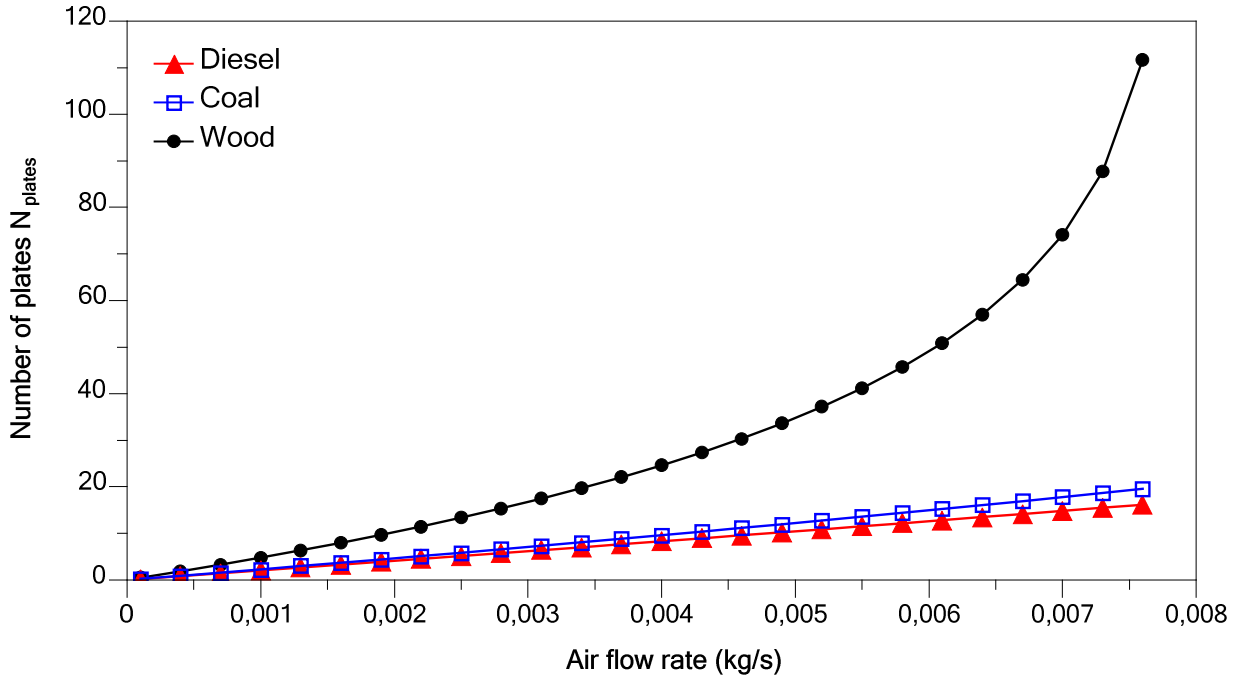


Figure 11. Number of plates required (N_{plate}).

The thermal energy of the exiting exhaust gases is in function of the gases exiting temperature. Figure 12 shows the effect of changing air flow rate on the energy remaining with exhaust gases. At 0.0001 kg/s flow rate of air, for wood fueled system, the heat rate at the outlet of the heat exchanger is 683.5 W, i.e. 6.5 W heat is transferred from exhaust gases to the air. Besides, at 0.0076 kg/s air flow rate, about 500 W of heat is delivered from the entering gases to air. Whereas, for Diesel the heat rate is 5.7 kW which decreases to 5.2 kW at 0.0001 kg/s and 0.0076 kg/s air flow rate respectively. While for coal, the heat rate at the outlet of the heat exchanger is 2.3 kW and decreases to 1.8 kW at 0.0001 kg/s and 0.0076 kg/s air flow rate respectively.

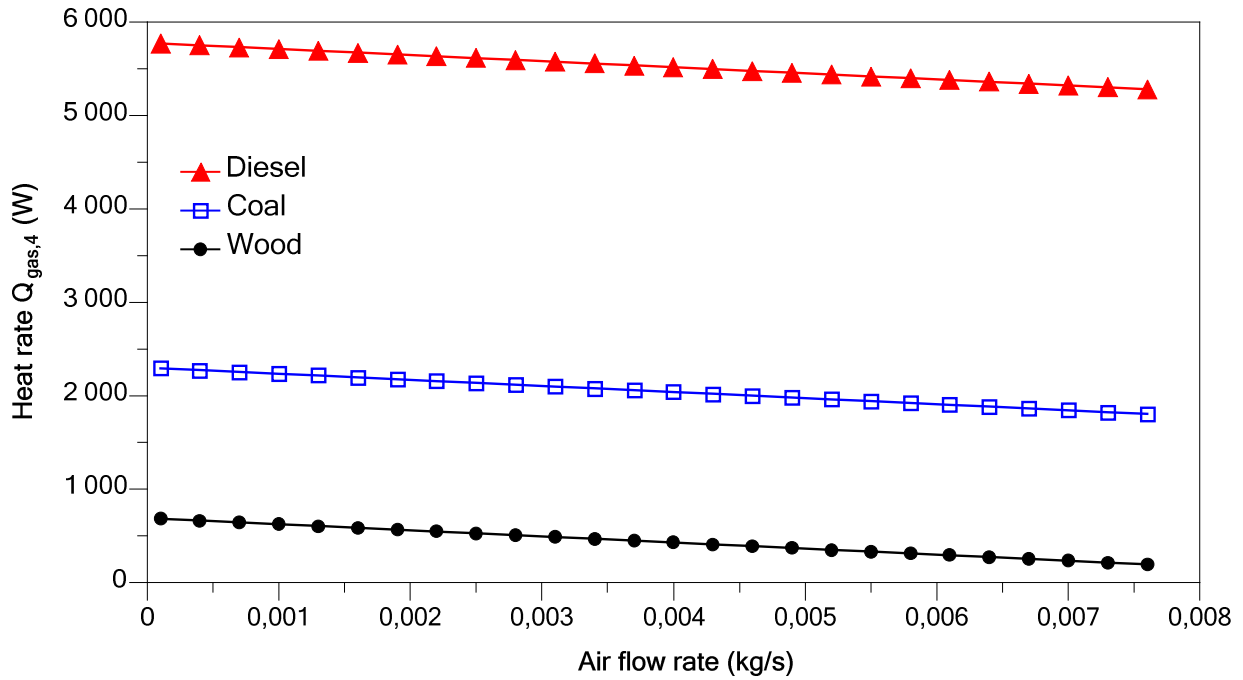


Figure 12. Heat rate at the outlet of the heat exchanger ($Q_{gas,4}$).

The energy recovery percentages at the HRHE are summarized in the Table 10 for the three different fuels used and three different air flow rates. For the maximum flow rate studied (0.0076 kg/s), only 8.5% of the diesel exhaust gases thermal energy is recovered, 21.5% for coal case and 71.7% for wood system. Therefore, for diesel or coal cases, more energy could be recovered by either increasing the mass flow rate of air or increasing the outlet air temperature (higher than 363 K).

Table 10. Percentage of energy recovery at the HRHE to the dryer.

Type of fuel	Percentage of energy recovery		
	$\dot{m}_a = 0.0001$ kg/s	$\dot{m}_a = 0.0043$ kg/s	$\dot{m}_a = 0.0076$ kg/s
Diesel	0.11%	4.8%	8.5%
Coal	0.2%	12.2%	21.5%
Wood	0.9%	40.5%	71.7%

4.5- Overall system

Figure 13 shows the variation of the exhaust gases temperature all over its pathway, at a constant mass flow rate of air 0.0076 kg/s. Coal system experiences higher decrease in exhaust gas temperature compared to diesel case knowing that coal combustion temperature is higher than diesel. This higher decrease is caused by the low mass flow rate of exhaust gases in the coal system compared to diesel one. Wood exhaust gases have the lowest burning temperature and lowest mass flow rate, which results by the lowest exit temperature ($T_{g,4}$). Since diesel has high mass flow rate and relatively high exhaust gases temperature, its exhaust gases temperature decreases slowly over the system: decrease of about 17.2% of the initial temperature. However, for coal case the exhaust gases temperature decreased of 33% and wood case has the highest temperature decrease of 58%.

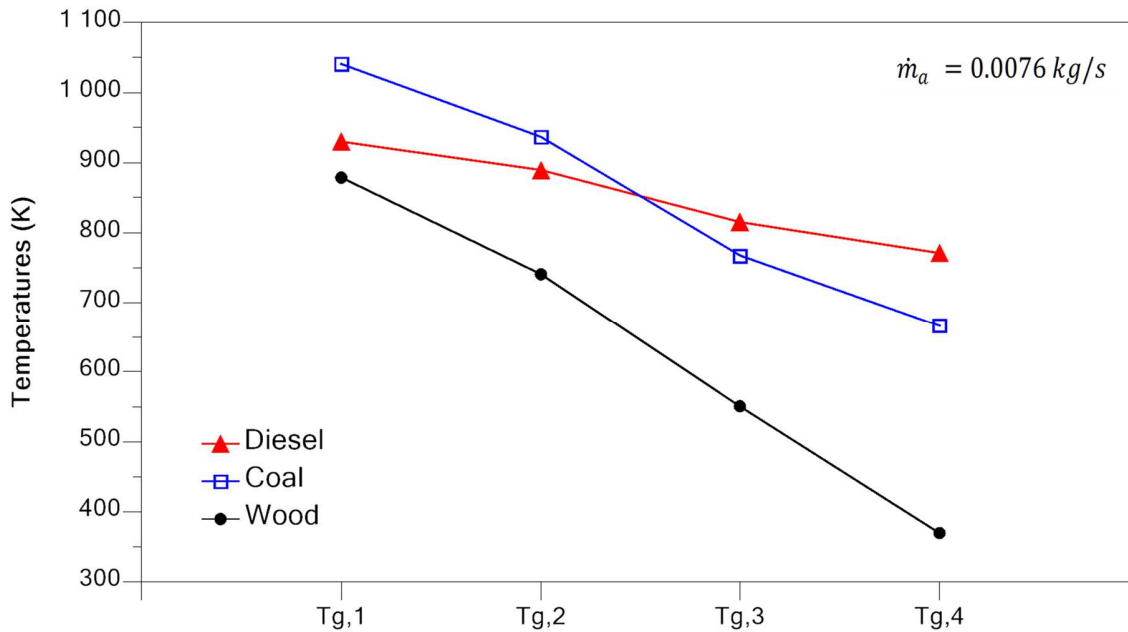


Figure 13. Exhaust gases temperature change over the system at $\dot{m}_a = 0.0076 \text{ kg/s}$.

Figure 14 shows the variation of the heat flow rate all over its pathway in the system, at a constant mass flow rate of air 0.0076 kg/s . When diesel is used it generated 7958 W and released 5282 W to environment while when coal is used, it produced 5269 W thermal energy and lost 1805 W to environment. For wood case it generated 2662 W thermal energy and rejected 194 W to environment. A part of the thermal energy generated from burning fuel is lost to ambient air inside room and part is recovered to heat domestic hot water, produce electricity and heat drying air to be utilized in a dryer, and the remaining part is lost to the environment.

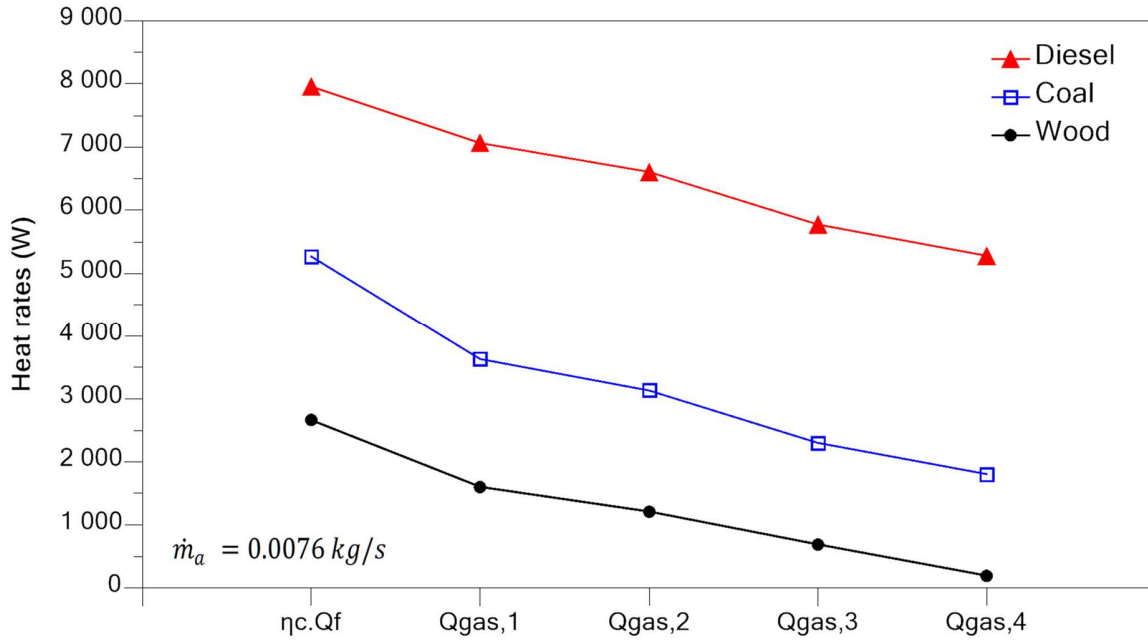


Figure 14. Heat flow rate change over the system at $\dot{m}_a = 0.0076 \text{ kg/s}$.

Since the main role of a chimney is to heat room's ambient air, then the thermal energy lost to the ambient air inside the room are not set as losses. The only thermal energy loss is the remaining thermal energy in exhaust gases (Q_{gas4}). Table 11 shows the percentage of useful and lost thermal energy from the produced thermal energy for the three types of fuel. Then it is compared to a conventional chimney system in which it consists only of chimney and pipe.

Table 11. Energy recovery from system.

Type of fuel	Designed chimney system (with heat recovery)		Conventional chimney system (without heat recovery)		% of energy recovered from lost energy
	% of energy used	% of energy lost	% of energy used	% of energy lost	
Diesel	34	66	17	83	20
Coal	66	34	41	59	42
Wood	93	7	54.5	45.5	84

When diesel is used to be the source of thermal energy in the chimney, it rejects the highest amount of thermal energy to the environment with or without heat recovery systems. However when using the heat recovery system, about 20% of the dissipated energy is being reused for producing hot water, hot air and electric power. For a conventional chimney that utilizes coal, 59% of the thermal energy generated is dissipated while when adding the heat recovery systems it rejects only 34% of its generated thermal energy. Wood chimneys are widely utilized and such system produces lower thermal energy due to the low heating value. When the wood chimney is connected with the heat recovery system, it only rejects 7% of its initial thermal energy: the heat recovery system recovers 84% of the dissipated energy.

Different types of fed fuel is studied and each scenario holds its outcomes. Table 12 below summarizes the scenarios results, shedding the light on the main results conducted, advantages and disadvantages of the heat recovery system.

Table 12. Main results, pros and cons of different scenarios considered in the study.

Case study	Main outputs	Advantages	Disadvantages
Diesel	<ul style="list-style-type: none"> ➤ 240 W electric power generated from TEGs ➤ 78°C hot water ➤ 90°C hot drying air at 0.0076 kg/s mass flow rate ➤ 0.16 m² heat exchanger area ➤ 20% of the dissipated energy is recovered 	<ul style="list-style-type: none"> ➤ Low risk for corrosion compared to other systems ➤ Produce high power ➤ Produce high water temperature ➤ Low amount of sticky flying ashes compared to coal and wood ➤ Lowest heat exchanger cost 	<ul style="list-style-type: none"> ➤ Low percentage of energy recovered ➤ Greater energy dissipated ➤ Diesel is more expensive than coal and wood
Coal	<ul style="list-style-type: none"> ➤ 240 W electric power generated from TEGs ➤ 78°C hot water ➤ 90°C hot drying air at 0.0076 kg/s mass flow rate ➤ 0.19 m² heat exchanger area ➤ 42% of the dissipated energy is recovered 	<ul style="list-style-type: none"> ➤ Produce high power ➤ Produce high water temperature ➤ Coal has low cost compared to diesel ➤ Low heat exchanger cost compared to wood 	<ul style="list-style-type: none"> ➤ High amount of ashes ➤ Risk of the pipe or heat exchanger closure resulted from ashes ➤ Risk of incomplete combustion resulted from trapping gases in the combustion chamber
Wood	<ul style="list-style-type: none"> ➤ 94 W electric power generated from TEGs ➤ 58°C hot water ➤ 90°C hot drying air at 0.0076 kg/s mass flow rate ➤ 1.11 m² heat exchanger area ➤ 84% of the dissipated energy is recovered 	<ul style="list-style-type: none"> ➤ Wood has low cost compared to diesel and coal ➤ High amount of energy recovered compared to other systems 	<ul style="list-style-type: none"> ➤ High amount of ashes ➤ Risk of the pipe or heat exchanger closure resulted from ashes ➤ Risk of incomplete combustion resulted from trapping gases in the combustion chamber ➤ High risk for corrosion (low gases temperature) ➤ High heat exchanger cost

The suggested triple heat recovery system has an overall efficiency of 63%, estimated by the summation of the used energy over the heat rate generated from the combustion of fuel. While Najjar and Kseibi [64] did a triple heat recovery system that generates electricity, cook and heat water, which has reached a 59% overall efficiency.

5- Conclusion

Multistage heat recovery from exhaust gases is an attractive growing field of study which is capturing the interest of scientists. The presented work suggests a new multistage heat recovery system that utilizes thermal energy released from combustion through exhaust gases to heat domestic water, generate electricity and heat air to be used in dryer. A complete thermal modeling of the system is illustrated starting from the equation of combustion till the released energy to environment. A case study is conducted in which three types of fuel (diesel, coal and wood) are studied and the results are analyzed and discussed. The main conclusions are drawn as follows:

- 1- At the furnace, the combustion of diesel, coal, and wood produced exhaust gases at temperature 930 K, 1041 K, 879 K respectively at a mass flow rate of 35.31 kg/hr, 15.44 kg/hr and 8.64 kg/hr respectively.
- 2- Heat loss from furnace walls are 11%, 30%, 40% of the initial thermal energy produced from burning of diesel, coal and wood respectively.
- 3- At the pipe, the energy loss through the wall of the pipe reduced the exhaust gases temperature by 3%, 9% and 15% of the diesel, coal, and wood exhaust gases.
- 4- The hybrid heat recovery system generated about 240 W for both diesel and coal cases, while it only produces 94 W for wood case.

5- The water at the tank is heated up to 351 K for diesel and coal cases, however when wood is used as fed fuel the water temperature increased to 331 K at steady state.

6- For a mass flow rate of air equal to 0.0076 kg/s, the area of the heat exchanger required is 0.16, 0.19 and 1.11 m² for diesel, coal and wood cases respectively.

7- The overall system recovered 20%, 42% and 84% of the energy dissipated to the environment for diesel, coal and wood cases respectively.

More thermal energy can be recovered for coal and diesel chimneys by increasing the volume of water, adding more layers of TEG, heating more air by either increasing air outlet temperature or by increasing the mass flow rate of the air, or even by adding a cooker.

References

- [1] C. Agrafiotis, T. Tsoutsos. Energy saving technologies in the European ceramic sector: a systematic review. *Applied Thermal Engineering*, 21, 2001, 1231-1249.
- [2] D. Zhang, J. Wang, Y. Lin, Y. Si, C. Huang, J. Yang, B. Huang, W. Li. Present situation and future prospect of renewable energy in China. *Renewable and Sustainable Energy Reviews*, 76, 2017, 865-871.
- [3] M. Mussard. Solar energy under cold climatic conditions: A review. *Renewable and Sustainable Energy Reviews*, 74, 2017, 733-745.
- [4] M. Ramadan, S. Ali, H. Bazzi, M.Khaled. New hybrid system combining TEG, condenser hot air and exhaust airflow of all-air HVAC systems. *Case Studies in Thermal Engineering*, 10, 2017, 154-160.
- [5] M. Khaled, M. Ramadan, H. El-Hage, A. Elmarakbi, F. Harambat, H. Peerhossaini. Review of underhood aerothermal management: Towards vehicle simplified models. *Applied Thermal Engineering*, 73, 1, 2014, 842-858.
- [6] M. Ramadan, M. Khaled, H. ElHage. Using Speed Bump for Power Generation –Experimental Study. *Energy Procedia*, 75, 2015, 867-872.
- [7] A.S. Ibanez-Lopez, B.Y. Moratilla-Soria. An assessment of Spain's new alternative energy support framework and its long-term impact on wind power development and system costs through behavioral dynamic simulation. *Energy*, 138, 2017, 629-646.
- [8] I.M. Sakr, Ali M. Abdelsalam, W.A. El-Askary. Effect of electrodes separator-type on hydrogen production using solar energy. *Energy*, 140, 2017, 625-632.
- [9] A. Herez, M. Ramadan, B. Abdulhay, M. Khaled. Short review on solar energy systems. *AIP Conference Proceedings*, 1758, Issue 1, 2016.
- [10] M. Ramadan, M. Khaled, H. S. Ramadan, M. Becherif. Modeling and sizing of combined fuel cell-thermal solar system for energy generation, accepted in the international journal for hydrogen energy.
- [11] L. Yang, E. Entchev, A. Rosato, S. Sibilio. Smart thermal grid with integration of distributed and centralized solar energy systems. *Energy*, 122, 2017, 471-481.
- [12] H. El Hage, A. Herez, M.Ramadan, H. Bazzi, M. Khaled. An investigation on solar drying: A review with economic and environmental assessment. *Energy*, 157, 2018, 815-829.
- [13] A. Herez, M. Ramadan, M. Khaled. Review on solar cooker systems: Economic and environmental study for different Lebanese scenarios. *Renewable and Sustainable Energy Reviews*, 81, 1, 2018, 421-432.
- [14] F. Hachem, B. Abdulhay, M. Ramadan, H. El Hage, M. Gad El Rab, M. Khaled. Improving the performance of photovoltaic cells using pure and combined phase change materials – Experiments and transient energy balance. *Renewable Energy*, 107, 2017, 567-575.
- [15] J. Dujardin, A. Kahl, B. Kruyt, S. Bartlett, M. Lehning. Interplay between photovoltaic, wind energy and storage hydropower in a fully renewable Switzerland. *Energy*, 135, 2017, 513-525.
- [16] A. Herez, M. Khaled, R. Murr, A. Haddad, H. Elhage, M. Ramadan. Using Geothermal Energy for cooling - Parametric study. *Energy Procedia*, 119, 2017, 783-791.
- [17] S. Tiwari, G. Tiwari. Energy and exergy analysis of a mixed-mode greenhouse-type solar dryer, integrated with partially covered N-PVT air collector. *Energy*, 128, 2017, 183-195.

- [18] J. Bosch, I. Staffell, A. Hawkes. Temporally-explicit and spatially-resolved global onshore wind energy potentials. *Energy*, 131, 2017, 207-217.
- [19] A. El Mays, R. Ammar, M. Hawa, M. Abou Akroush, F. Hachem, M. Khaled, M. Ramadan. Improving Photovoltaic Panel Using Finned Plate of Aluminum. *Energy Procedia*, 119, 2017, 812-817.
- [20] J. Atherton, R. Sharma, J. Salgado. Techno-economic analysis of energy storage systems for application in wind farms. *Energy*, 135, 2017, 540-552.
- [21] M.F Remeli, K. Verojporn, B. Singh, L. Kiatbodan, A. Date, A. Akbarzadeh. Passive Heat Recovery System using Combination of Heat Pipe and Thermoelectric Generator. *Energy Procedia*, 75, 2015, 608-614.
- [22] H. Jaber, M. Khaled, T. Lemenand, J. Faraj, H. Bazzi, M. Ramadan. Effect of Exhaust Gases Temperature on the Performance of a Hybrid Heat Recovery System. *Energy Procedia*, 119, 2017, 775-782.
- [23] S. Shen, W. Cai, X. Wang, Q. Wu, H. Yon. Investigation of liquid desiccant regenerator with fixed-plate heat recovery system. *Energy*, 137, 2017, 172-182.
- [24] S. Bellocchi, G. Guizzi, M. Manno, M. Pentimalli, M. Salvatori, A. Zaccagnini. Adsorbent materials for low-grade waste heat recovery: Application to industrial pasta drying processes. *Energy*, 140, 2017, 729-745.
- [25] R. Mal, R. Prasad, V.K. Vijay. Renewable Energy from Biomass Cookstoves for Off Grid Rural Areas. *International Congress on Environmental, Biotechnology, and Chemistry Engineering*, 64, 2014, 21.
- [26] A. El Mays, R. Ammar, M. Hawa, M. Abou Akroush, F. Hachem, M. Khaled, M. Ramadan. Using phase change material in under floor heating. *Energy Procedia*, 119, 2017, 806-811.
- [27] F. Meng, L. Chen, Y. Feng, B. Xiong. Thermoelectric generator for industrial gas phase waste heat recovery. *Energy*, 135, 2017, 83-90.
- [28] T. Eller, F. Heberle, D. Brüggemann. Second law analysis of novel working fluid pairs for waste heat recovery by the Kalina cycle. *Energy*, 119, 2017, 188-198.
- [29] M. Ramadan, T. Lemenand, M. Khaled. Recovering heat from hot drain water—Experimental evaluation, parametric analysis and new calculation procedure. *Energy and Buildings*, 128, 2016, 575-58.
- [30] R. Carapellucci, L. Giordano. The Recovery of Exhaust Heat from Gas Turbines, Department of Mechanical, Energy and Management Engineering University of L'Aquila Italy.
- [31] M. Khaled, M. Ramadan. Study of the thermal behavior of multi concentric tube tank in heat recovery from chimney – Analysis and optimization. *Heat Transfer Engineering Journal*, 8, 1-11, 2017.
- [32] B. Zalba, J. Marin, L.F. Cabeza, H. Mehling. Review on thermal energy storage with phase change: materials, heat transfer analysis and applications. *Applied Thermal Engineering*, 23, 2003, 251-283.
- [33] M. Khaled, M. Ramadan. Heating fresh air by hot exhaust air of HVAC systems. *Case Studies in Thermal Engineering*, 8, 2016, 398-402.
- [34] T. Hu, X. Xie, Y. Jiang. Simulation research on a variable-lift absorption cycle and its application in waste heat recovery of combined heat and power system. *Energy*, 140, 2017, 912-921.
- [35] A. Mezquita, J. Boix, E. Monfort, G. Mallol. Energy saving in ceramic tile kilns: Cooling gas heat recover. *Applied Thermal Engineering*, 65, 2014, 102-110.

- [36] M. Wei, W. Yuan, Z. Song, L. Fu, S. Zhang. Simulation of a heat pump system for total heat recovery from flue gas. *Applied Thermal Engineering*, 86, 2015, 326-332.
- [37] M. Khaled, M. Ramadan, H. El Hage. Innovative approach of determining the overall heat transfer coefficient of heat exchangers – Application to cross-flow water-air types. *Applied Thermal Engineering*, 99, 2016, 1086-1092.
- [38] R. Morgan, G. Dong, A. Panesar, M. Heikal. A comparative study between a Rankine cycle and a novel intra-cycle based waste heat recovery concepts applied to an internal combustion engine. *Applied Energy*, 174, 2016, 108-117.
- [39] D. Lee, J. Park, M. Ryu, J. Park. Development of a highly efficient low-emission diesel engine-powered co-generation system and its optimization using Taguchi method. *Applied Thermal Engineering*, 50, 2013, 491-495.
- [40] Z. Song, J. Chen, L. Yang. Heat transfer enhancement in tubular heater of Stirling engine for waste heat recovery from flue gas using steel wool. *Applied Thermal Engineering*, 87, 2015, 499-504.
- [41] H. Jaber, M. Khaled, T. Lemenand, M. Ramadan. Short review on heat recovery from exhaust gas. *AIP Conference Proceedings*, 1758, Issue 1, 2016, 10.1063/1.4959441.
- [42] M. Khaled, M. Ramadan, H. El Hage. Parametric Analysis of Heat Recovery from Exhaust Gases of Generators. *Energy Procedia*, 75, 2015, 3295-3300.
- [43] M. Hatami, D. Ganji, M. Gorji-Bandpy. A review of different heat exchangers designs for increasing the diesel exhaust waste heat recovery. *Renewable and Sustainable Energy Reviews*, 37, 2014, 168–181.
- [44] P. Zhang, T. Ma, W. Li, G. Ma, Q. Wang. Design and optimization of a novel high temperature heat exchanger for waste heat cascade recovery from exhaust flue gases. *Energy*, 160, 2018, 3-18.
- [45] M. Khaled, M. Ramadan, K. Chahine, A. Assi. Prototype implementation and experimental analysis of water heating using recovered waste heat of chimneys. *Case Studies in Thermal Engineering*, 5, 2015, 127–133.
- [46] E. Elgendy, J. Schmidt. Optimum utilization of recovered heat of a gas engine heat pump used for water heating at low air temperature. *Energy and Buildings*, 80, 2014, 375-383.
- [47] K. Tanha, A. S. Fung, R. Kumar. Performance of two domestic solar water heaters with drain water heat recovery units: Simulation and experimental investigation. *Applied Thermal Engineering*, 90, 2015, 444-459.
- [48] M. Ramadan, M. Gad El Rab, M. Khaled. Parametric analysis of air–water heat recovery concept applied to HVAC systems: Effect of mass flow rates. *Case Studies in Thermal Engineering*, 6, 2015, 61–68.
- [49] M. Remeli, L. Tan, A. Date, B. Singh, A. Akbarzadeh. Simultaneous power generation and heat recovery using a heat pipe assisted thermoelectric generator system. *Energy Conversion and Management*, 91, 2015, 110–119
- [50] G. Huang, C. Hsu, C. Fang, D. Yao. Optimization of a waste heat recovery system with thermoelectric generators by three-dimensional thermal resistance analysis. *Energy Conversion and Management*, 126, 2016, 581–594.
- [51] M. Demira, I. Dincera. Development and heat transfer analysis of a new heat recovery system with thermoelectric generator. *International Journal of Heat and Mass Transfer*, 108, 2017, 2002–2010.
- [52] T. Kim, A. Negash, G. Cho. Experimental and numerical study of waste heat recovery characteristics of direct contact thermoelectric generator. *Energy Conversion and Management*, 140, 2017, 273–280.

- [53] M Remeli, A. Date, B. Orr, L. Ding, B. Singh, N. Affandi, A. Akbarzadeh. Experimental investigation of combined heat recovery and power generation using a heat pipe assisted thermoelectric generator system. *Energy Conversion and Management*, 111, 2016, 147–157.
- [54] D. Madan, Z. Wang, P. Wright, J. Evans. Printed flexible thermoelectric generators for use on low levels of waste heat. *Applied Energy*, 156, 2015, 587–592.
- [55] G. Shu, X. Ma, H. Tian, H. Yang, T. Chen, X. Li. Configuration optimization of the segmented modules in an exhaust-based thermoelectric generator for engine waste heat recovery. *Energy*, 160, 2018, 612-624.
- [56] A. Nour Eddine, D. Chalet, X. Faure, L. Aixala, P. Chessé. Effect of engine exhaust gas pulsations on the performance of a thermoelectric generator for wasted heat recovery: An experimental and analytical investigation. *Energy*, 162, 2018, 715-727.
- [57] M. Tańczuk, W. Kostowski, M. Karaś. Applying waste heat recovery system in a sewage sludge dryer – A technical and economic optimization. *Energy Conversion and Management*, 125, 2016, 121-132.
- [58] X. Han, J. Yan, S. Karellas, M. Liu, E. Kakaras, F. Xiao. Water extraction from high moisture lignite by means of efficient integration of waste heat and water recovery technologies with flue gas pre-drying system. *Applied Thermal Engineering*, 110, 2017, 442-456.
- [59] T. Walmsley, M. Walmsley, M. Atkins, J. Neale, A. Tarighaleslami. Thermo-economic optimisation of industrial milk spray dryer exhaust to inlet air heat recovery. *Energy*, 90, 2015, 95–104.
- [60] J. Pati, S. Hotta, P. Mahanta. Effect of Waste Heat Recovery on Drying Characteristics of Sliced Ginger in a Natural Convection Dryer. *Procedia Engineering*, 105, 2015, 145-152.
- [61] B. Golman, W. Julklang. Simulation of exhaust gas heat recovery from a spray dryer. *Applied Thermal Engineering*, 73, 2014, 899–913.
- [62] Q. Jian, L. Luo. The improvement on efficiency and drying performance of a domestic venting tumble clothes dryer by using a heat pipe heat recovery heat exchanger. *Applied Thermal Engineering*, 136, 2018, 560-567.
- [63] H. Jaber, M. Ramadan, T. Lemenand, M. Khaled. Domestic thermoelectric cogeneration system optimization analysis, energy consumption and CO2 emissions reduction. *Applied Thermal Engineering*, 130, 2018, 279–295.
- [64] Y.S.H. Najjar, M.M. Kseibi. Heat transfer and performance analysis of thermoelectric stoves. *Applied Thermal Engineering*, 102, 2016, 1045–1058.
- [65] F.P. Incorpera, D.P. DeWitt. 2007. *Fundamentals of heat and mass transfer*. Sixth Edition. John Wiley & Sons.